CD44 knockdown and TGF-β inhibition modulate cell proliferation and invasion in claudin-low breast cancer cells

RYOICHI MATSUNUMA[1], KAZUO KINOSHITA[2], SAE IMADA[1], SHOKO SATO[1], RYOSUKE HAYAMI[1] and MICHIKO TSUNEIZUMI[1]

[1]Department of Breast Surgery, Shizuoka General Hospital, Shizuoka, Shizuoka 420-8527, Japan; [2]Evolutionary Medicine, Shizuoka Graduate University of Public Health, Shizuoka, Shizuoka 420-0881, Japan

Received May 24, 2025; Accepted October 3, 2025

DOI: 10.3892/or.2025.9012

Abstract. CD44 serves a dual role in supporting tumor survival and promoting invasion. Claudin-low breast cancer, characterized by a $CD44^+/CD24^-$ phenotype and epithelial-mesenchymal transition (EMT), displays aggressive behavior. The present study investigated the interaction between CD44 and TGF-β signaling, and assessed the cellular effects of their combined inhibition. CD44 was knocked down in claudin-low breast cancer cell lines (SUM159 and MDA-MB-231), and the TGF-β receptor (TGFBR) inhibitor LY2109761 (LY-61) was applied for treatment. Cell viability (MTT assay), apoptosis (annexin V assay), invasion (Transwell assay), colony formation and Smad2 phosphorylation (western blotting) were evaluated. CD44 knockdown reduced viability and increased apoptosis but did not markedly suppress invasion. Although TGF-β stimulation enhanced Smad2 phosphorylation, CD44 knockdown alone did not increase Smad2 activation, indicating that it does not directly regulate Smad2. However, LY-61 inhibited TGF-β-induced Smad2 phosphorylation, effectively counteracting pro-invasive signaling. Notably, while CD44 knockdown alone had a negligible impact on invasion, its combination with LY-61 markedly reduced the invasive capacity and colony formation of cells compared with the control (control cells transduced with non-targeting short hairpin RNA without LY-61 treatment). LY-61 induced S phase accumulation, which was more pronounced in SUM159 cells than in MDA-MB-231 cells, indicating cell line-specific effects on cell-cycle regulation. Clinical data indicated that low CD44 expression was associated with improved survival in patients with claudin-low breast cancer, despite its potential to enhance EMT signaling. These findings suggested that CD44 knockdown enhanced the response to TGFBR inhibition. Although CD44 depletion may increase EMT-related signaling, invasion was primarily suppressed by TGF-β blockade, and the combination with CD44 knockdown further enhanced the inhibition of proliferative phenotypes compared with either treatment alone. This dual-targeting approach warrants further investigation in claudin-low breast cancer.

Correspondence to: Dr Ryoichi Matsunuma, Department of Breast Surgery, Shizuoka General Hospital, 4-27-1 Kita-ando, Aoi-ku, Shizuoka, Shizuoka 420-8527, Japan
E-mail: r-matsunuma@nifty.com

Key words: CD44, TGF-β, claudin-low breast cancer

Introduction

Breast cancer is a heterogeneous disease that comprises multiple intrinsic subtypes, each associated with distinct clinical and molecular characteristics (1). Based on gene expression profiling, four major intrinsic subtypes (luminal A, luminal B, HER2-enriched and basal-like) have traditionally been identified (2,3). These classifications guide treatment and provide insights into prognosis (4). However, a novel intrinsic subtype, termed claudin-low, was identified in 2007 (5). Claudin-low breast cancers are unique due to their low expression of claudins, which are tight junction adhesion molecules integral to epithelial cell cohesion and polarity. As a result, claudin-low tumors exhibit characteristics more typical of mesenchymal cells, including increased motility and invasiveness. These properties are associated with high expression levels of epithelial-mesenchymal transition (EMT) markers, reflecting an inherently aggressive phenotype (6-8).

Over 70% of claudin-low breast cancers are also classified as triple-negative, which means that they lack estrogen receptor, progesterone receptor and HER2 expression. This renders claudin-low tumors resistant to conventional endocrine or HER2-targeted therapies, limiting the treatment options for this subtype. Beyond the distinctive expression of claudins and EMT markers, claudin-low tumors share features with cancer stem cells, such as a $CD44^+/CD24^-$ surface marker profile (9). This $CD44^+/CD24^-$ phenotype is linked to cancer stem cell-like traits such as self-renewal and chemoresistance, contributing to poor clinical outcomes (6,7).

The CD44 protein, a cell surface glycoprotein involved in cell-cell and cell-matrix interactions, has been implicated in various aspects of cancer biology, including cell proliferation, invasion and metastasis (10). In CD44-positive breast cancer cells, studies have reported that CD44 inhibition can suppress cell proliferation and, in some cases, diminish invasive capabilities (11-14). However, the results regarding invasion are varied; while some studies have suggested that CD44

inhibition can limit invasiveness (15,16), others have reported negligible effects on invasion (17,18). This variation may stem from the complex involvement of CD44 in multiple signaling pathways that collectively influence cell behavior in diverse mechanisms. Despite these inconsistencies, the evidence highlights the substantial role of CD44 in promoting the aggressive characteristics of claudin-low breast cancers, particularly through its regulatory impact on EMT processes (19,20).

EMT is a cellular program that drives epithelial cells to acquire mesenchymal properties, enhancing their migratory and invasive capabilities. EMT inhibition in claudin-low breast cancer may offer dual benefits: Cell motility reduction and tumor growth suppression (21,22). By targeting the EMT pathway, certain inhibitors, such as histone deacetylase inhibitors and DNA methyltransferase inhibitors, could theoretically control the proliferation and metastatic potential of claudin-low breast cancers (23). However, studies suggest that EMT inhibition alone provides only limited therapeutic benefits, indicating a need for combination therapies that target multiple pathways (24,25). This observation has driven further research into the identification of co-targets that may enhance the efficacy of EMT inhibitors.

Previous findings have indicated that the TGF-β receptor (TGFBR), an upstream EMT regulator, can directly interact with CD44, providing a novel therapeutic axis for claudin-low breast cancers (26). Given the interplay between CD44 and TGF-β signaling, the dual inhibition of CD44 and TGFBRs may amplify the antiproliferative and anti-invasive effects of single-agent treatments (23). Pharmacological agents that downregulate CD44 expression and inhibit TGF-β signaling could, therefore, provide a combined approach, targeting the EMT pathway while impacting the CD44-mediated stem cell-like properties of claudin-low breast cancers (27,28). This combined approach may provide a mechanistic rationale for co-targeting CD44 and TGF-β signaling, as CD44 interacts with the TGF-β receptor complex, modulating downstream Smad2 activation. Dual inhibition could simultaneously suppress CD44-mediated stem cell-like survival and TGF-β-driven EMT and invasion, thereby enhancing antiproliferative efficacy in claudin-low breast cancer.

Materials and methods

Antibodies. The antibodies used in the present study were anti-CD44 (1:1,000; cat. no. sc-7297; Santa Cruz Biotechnology, Inc.), anti-Smad2 (1:1,000; cat. no. 3102; Cell Signaling Technology, Inc.), anti-phosphorylated (p-)Smad2 (Ser465/467) (1:1,000; cat. no. 3108; Cell Signaling Technology, Inc.), anti-TGFBR1 (1:1,000; cat. no. sc-101574; Santa Cruz Biotechnology, Inc.), anti-TGFBR2 (1:1,000; cat. no. sc-17799; Santa Cruz Biotechnology, Inc.), anti-Bcl-2 (1:1,000; cat. no. sc-7382; Santa Cruz Biotechnology, Inc.), anti-Snai1 (1:1,000; cat. no. sc-271977; Santa Cruz Biotechnology, Inc.), anti-IgG (1:10,000; cat. no. 5415; Cell Signaling Technology, Inc.) and anti-GAPDH (1:1,000; cat. no. sc-32233; Santa Cruz Biotechnology, Inc.).

Cell culture and lentiviral transduction. The MDA-MB-231, SUM159 and MDA-MB-468 human breast cancer cell lines were obtained from stocks maintained at Shizuoka General Hospital (Shizuoka, Japan). MDA-MB-231 and MDA-MB-468 cells were maintained in DMEM (Nacalai Tesque, Inc.) supplemented with 10% FBS (Biowest) and 1% penicillin-streptomycin (100 U/ml penicillin and 100 μg/ml streptomycin). SUM159 cells were maintained in Ham's F-12 medium (Gibco; Thermo Fisher Scientific, Inc.) supplemented with 5% FBS (Biowest), 5 μg/ml insulin (Sigma-Aldrich; Merck KGaA) and 1 μg/ml hydrocortisone (Sigma-Aldrich; Merck KGaA). All cells were cultured at 37˚C in a humidified incubator containing 5% CO_2. These cell lines were confirmed to be free of mycoplasma contamination and exhibited morphological features consistent with previously reported characteristics [MDA-MB-231 and MDA-MB-468 cells: American Type Culture Collection; SUM159 cells: (29)]. SUM159 and MDA-MB-231 have previously been classified as claudin-low breast cancer cell lines, while MDA-MB-468 has been classified as a basal-like breast cancer cell line (6,25).

CD44 knockdown was performed using short hairpin RNA (shRNA/sh; TRCN0000296191; Sigma-Aldrich; Merck KGaA), which targeted the sequence 5'-GGACCAATTACC ATAACTATT-3' (sense strand). The corresponding antisense strand was 5'-AATAGTTATGGTAATTGGTCC-3'. The shRNA was cloned into the pLKO.1-puro lentiviral vector (MISSION pLKO.1-puro; Sigma-Aldrich; Merck KGaA), which expressed the shRNA under the control of the U6 promoter and included a puromycin resistance gene for stable selection. MISSION pLKO.1-puro non-target shRNA control plasmid DNA (SHC016; Sigma-Aldrich; Merck KGaA) was used as an appropriate control. The sense strand of the control shRNA was 5'-GCGCGATAGCGCTAATAATTT-3', and the corresponding antisense strand was 5'-AAATTATTA GCGCTATCGCGC-3'. Lentiviral particles were produced in 293 cells (institutional stock; Shizuoka General Hospital, Shizuoka, Japan) using a second-generation packaging system (MISSION Lentiviral Packaging Mix; Sigma-Aldrich; Merck KGaA) and FuGENE HD transfection reagent (Promega Corporation). For each 10-cm dish, 2.6 μg pLKO.1-puro transfer plasmid, 26 μl MISSION Lentiviral Packaging Mix and 16 μl FuGENE HD were combined according to the manufacturers' instructions and added to cells at 37˚C. After 24 h, the medium was replaced with fresh growth medium. Viral supernatants were harvested at 48 and 72 h post-transfection and passed through a 0.45-μm filter. MDA-MB-231 and SUM159 cells were transduced at an MOI of 5 in the presence of 8 μg/ml polybrene for 24 h. Stable transductants were selected with puromycin (1.0 μg/ml) for 5 days, followed by culture in puromycin-free medium for 72 h to allow recovery and to minimize cytotoxic stress associated with prolonged antibiotic exposure, after which downstream assays were performed.

RNA extraction and reverse transcription-quantitative PCR (RT-qPCR). Total RNA was extracted from each cell line using the RNeasy Mini Kit (Qiagen KK) according to the manufacturer's protocol. RNA was reverse-transcribed into cDNA using the iScript cDNA Synthesis Kit (Bio-Rad Laboratories, Inc.) in a 20-μl reaction according to the manufacturer's protocol. Equal cDNA amounts were used as templates for RT-qPCR to detect mRNA expression relative to that of GAPDH (endogenous control). mRNA expression was quantitated using a

Thermal Cycler Dice® Real Time System III (Takara Bio, Inc.) and SYBR-Green qPCR SuperMix (Invitrogen; Thermo Fisher Scientific, Inc.). The thermocycling conditions were as follows: Initial denaturation at 95˚C for 30 sec, followed by 40 cycles of 95˚C for 15 sec and 60˚C for 30 sec. Melting curve analysis was performed to verify product specificity. The primers used were: *Smad2* forward, 5'-AGTGTGTAAAATTCCACC AG-3' and reverse, 5'-ATTCTAGTTAGCTGATAGACGG-3'; *GAPDH* forward, 5'-TCGGAGTCAACGGATTTG-3' and reverse, 5'-GCAACAATATCCACTTTACCAGAG-3'; snail family transcriptional repressor 1 (*Snai1*) forward, 5'-CTC TAATCCAGAGTTTACCTTC-3' and reverse, 5'-GACAGA GTCCCAGATGAG-3'; and *Twist* forward, 5'-CTAGATGTC ATTGTTTCCAGAG-3' and reverse, 5'-CCCTGTTTCTTT GAATTTGG-3'. RT-qPCR reactions were performed in triplicate, and each experiment was repeated three times. The fold induction of gene expression was calculated using the $2^{-\Delta\Delta Cq}$ method (30).

Immunoprecipitation and western blotting. Cells were lysed in RIPA buffer (50 mM Tris-HCl, pH 7.4; 150 mM NaCl; 1% NP-40; 0.5% sodium deoxycholate; 0.1% SDS) supplemented with protease and phosphatase inhibitors (Roche Diagnostics GmbH). For each immunoprecipitation, 50 μl Dynabeads Protein G magnetic beads (Invitrogen; Thermo Fisher Scientific, Inc.) were pre-incubated with 3 μg of the indicated primary antibody (anti-CD44; cat. no. sc-7297; Santa Cruz Biotechnology, Inc.) or normal mouse IgG (cat. no. 5415; Cell Signaling Technology, Inc.) for 30 min at room temperature with gentle rotation to allow formation of bead-antibody complexes. Subsequently, 500 μg lysate was added to the bead-antibody complexes and samples were incubated for 1 h at room temperature with rotation. The immune complexes were isolated magnetically using a DynaMag™-2 magnet (Thermo Fisher Scientific, Inc.) and washed three times with PBS at room temperature. Bound proteins were eluted by boiling the beads in 2X Laemmli sample buffer (Bio-Rad Laboratories, Inc.) for 5 min, resolved via SDS-PAGE and transferred onto nitrocellulose membranes. Western blotting was performed using specific antibodies as previously described (31). These conditions were applied to all western blot experiments performed in the present study. For the analysis of TGF-β-induced Smad2 phosphorylation, cells were treated with recombinant human TGF-β1 (10 ng/ml; PeproTech, Inc.; Thermo Fisher Scientific, Inc.) at 37˚C for 2 h prior to protein extraction, unless otherwise specified.

Cell cycle analysis. Cells ($2x10^5$ cells/well) were seeded in 6-well plates and incubated at 37˚C in a humidified atmosphere with 5% CO_2 for 24 h. Subsequently, the cells were treated with 10 μM LY2109761 (LY-61; Selleck Chemicals) at 37˚C for 48 h. After trypsinization, the cells were fixed and stained according to the protocol of the Cell Cycle Phase Determination Kit (item no. 10009349; Cayman Chemical Company). The cell cycle distribution was analyzed via flow cytometry using a BD FACSMelody™ flow cytometer (BD Biosciences). Propidium iodide fluorescence was detected in the BP/700/54 channel with a blue laser, and data were analyzed using BD FACSChorus software (version 1.3.2; BD Biosciences). Cell cycle phase distributions (G_1, S and G_2/M) were calculated using FlowJo software (version 10.10.0; BD Biosciences).

Apoptosis assay. Apoptosis was analyzed according to the protocol from BioLegend, Inc. After a 48-h incubation at 37˚C in a humidified atmosphere with 5% CO_2 in either standard media or media containing 10 μM LY-61, the cells were washed twice with cold Cell Staining Buffer (cat. no. 420201; BioLegend, Inc.) and resuspended in Annexin V Binding Buffer (cat. no. 422201; BioLegend, Inc.) at a concentration of $1x10^6$ cells/ml. A 100-μl aliquot of the cell suspension was transferred into a 5-ml test tube, and 5 μl FITC-conjugated Annexin V (cat. no. 640906; BioLegend, Inc.) and 5 μl 7-aminoactinomycin D (7-AAD; cat. no. 420403; BioLegend, Inc.) were added simultaneously. Subsequently, the cells were incubated in the dark for 15 min at room temperature. After incubation, 400 μl Annexin V Binding Buffer was added to each sample prior to flow cytometry analysis. Fluorescence signals were detected using a BD FACSMelody™ flow cytometer (BD Biosciences) equipped with a 488-nm blue laser, detecting FITC fluorescence in the BP/530/40 channel and 7-AAD fluorescence in the BP/700/54 channel. Data were acquired and analyzed using BD FACSChorus software (version 1.3.2; BD Biosciences), and data were processed with FlowJo software (version 10.10.0; BD Biosciences).

MTT assay. MTT assays were performed using the MTT Cell Proliferation and Cytotoxicity Assay Kit (AR1156; Boster Bio). A total of 1,000 cells per well were seeded in 96-well cell culture plates, and the assay was performed according to the manufacturer's protocol. After incubation with 10 μl MTT labeling reagent for 4 h, 100 μl Formazan Solubilization Solution (included in the kit; Boster Bio) was added to each well, and the plate was further incubated at 37˚C for 4-18 h to ensure complete dissolution of the purple formazan crystals. The absorbance was measured at 560 nm using a microplate reader. Cell viability was quantified on day 5 post-plating, and the relative viability was calculated as the ratio of absorbance values on day 5.

Clonogenic assay. A total of 500 cells per well were seeded in 6-well plates and allowed to attach overnight. MDA-MB-231 and SUM159 cells were cultured in standard media or media containing 10 μM LY-61 at 37˚C with 5% CO_2 for 7 days. The colonies were fixed with 4% paraformaldehyde (FUJIFILM Wako Pure Chemical Corporation) at room temperature for 15 min, stained with 0.5% crystal violet at room temperature for 20 min and washed with distilled water. Colonies (diameter >0.5 mm) were counted manually under a light microscope.

Invasion assay. The invasiveness of MDA-MB-231 and SUM159 cells was evaluated using the CytoSelect™ 24-well Cell Invasion Assay Kit (cat. no. CBA-110; Cell Biolabs, Inc.) according to the manufacturer's protocols. Transwell inserts with polycarbonate membranes (8-μm pore size) were precoated with Matrigel at 37˚C for 2 h, and the Matrigel layer was rehydrated at room temperature for 1 h before cell seeding. For the invasion assay, MDA-MB-231 cells were maintained in DMEM (Nacalai Tesque, Inc.) and SUM159

cells were maintained in Ham's F-12 medium (Nacalai Tesque, Inc.) as aforementioned. A total of $2x10^5$ cells in 300 μl of the corresponding serum-free medium were added to the upper chamber, while 500 μl of the same medium containing 10% FBS (Biowest, distributed by Funakoshi Co., Ltd.) with or without 10 μM LY-61 was placed in the lower chamber as a chemoattractant. After incubation at 37˚C in 5% CO_2 for 48 h, non-invading cells were removed, and invaded cells were stained with the dye solution provided in the kit at room temperature for 10 min. Stained samples (100 μl) from each well were transferred to a 96-well plate, and absorbance was measured at 560 nm using a microplate reader. Representative images of invaded cells were captured using a Nikon ECLIPSE TS2 light microscope (Nikon Corporation).

Statistical analysis. Statistical analyses were conducted using GraphPad Prism® version 10.3.1 (Dotmatics) and Microsoft® Excel Version 2019 (Microsoft Corporation). All data are presented as the mean ± SD from at least three independent experiments. Data normality was assessed using the Shapiro-Wilk test. For normally distributed data, statistical comparisons among multiple groups were conducted using one-way or two-way ANOVA followed by Tukey's or Dunnett's multiple comparisons test, as appropriate. Unpaired two-tailed Student's t-tests were used for pairwise comparisons. For non-normally distributed data (such as mutation burden data), statistical comparisons between two groups were performed using the Mann-Whitney U test. $P<0.05$ was considered to indicate a statistically significant difference.

Public dataset analysis. Genomic and clinical data, including copy number alterations (CNAs) and mRNA expression levels, were obtained from the METABRIC dataset via cBioPortal (https://www.cbioportal.org/). Frequencies of CNAs for selected genes were summarized according to breast cancer subtype using the cBioPortal interface. Kaplan-Meier survival analyses were performed in GraphPad Prism using mRNA expression z-scores and associated clinical outcome data from the METABRIC cohort. Patients were divided into high and low expression groups based on the median value, and P-values were calculated using the log-rank test. No additional statistical software or custom computational pipelines were used. Data from the METABRIC study were originally published by Curtis *et al* (32).

Protein-protein interaction (PPI) network analysis. PPI networks were analyzed using the STRING database (version 11.0; https://string-db.org) (33). Interactions with a medium confidence score (>0.4) were included.

Results

Genomic alterations in claudin-low breast cancer: CNA-driven therapeutic implications of CD44, TGFBR1 and TGFBR2. Breast cancer is a heterogeneous disease that comprises molecular subtypes with distinct genetic and phenotypic profiles (2,3). CNAs and somatic mutations are crucial in promoting oncogenesis, as well as influencing tumor progression and therapeutic response (9,34). Among the key genes, CD44, a cancer stem cell marker, and TGFBR1/2, which mediate TGF-β signaling (24,35), are implicated in tumor invasion and metastasis (36). The presence of CNAs in these genes suggests that their dysregulation may create potential therapeutic vulnerabilities, genetic dependencies that could be exploited for targeted intervention in claudin-low breast cancer.

CD44, TGFBR1 and TGFBR2 exhibited similar CNA patterns, characterized by moderate deletion frequencies and rare amplifications across all subtypes. In the claudin-low subtype, their deletion frequencies were intermediate, ranking third or fourth highest among all breast cancer subtypes (generally <10% for CD44 and 10-15% for TGFBR1/2). By contrast, BRCA1 and BRCA2 displayed higher alteration rates, with basal-like tumors showing prominent deletion frequencies (~40%) (Fig. 1A). This highlights the unique genomic roles of CD44, TGFBR1 and TGFBR2 in tumor biology, which are distinct from BRCA1/2.

Genome-wide mutation analysis (Fig. 1B) revealed a statistically significant difference in the mutational burden between claudin-low and basal subtypes, which are both representatives of triple-negative breast cancer (TNBC). Claudin-low tumors exhibited a lower mutational burden (mean, 4.43±2.70; n=179) compared with basal tumors (mean, 6.39±3.84; n=197), and this difference was confirmed by a Mann-Whitney U test ($P<0.0001$). These findings suggested that claudin-low tumors rely more on CNAs or epigenetic changes than on mutations.

By contrast, basal tumors exhibited a broader distribution of mutation counts and higher average burden, consistent with known genomic instability in this subtype. Such instability is frequently associated with defects in DNA damage response pathways, including BRCA1/2 mutations, and may contribute to the aggressive phenotype characteristic of basal-like TNBC (9,34).

CD44, TGFBR1 and TGFBR2 displayed negligible mutation frequencies across all subtypes in the METABRIC dataset (data not shown), suggesting they are more commonly affected by CNAs rather than point mutations in claudin-low tumors.

The similar CNA patterns observed in CD44, TGFBR1 and TGFBR2 suggest a potentially coordinated regulatory mechanism, possibly linked to pathways that drive tumor progression. In claudin-low tumors, which exhibit a lower overall mutational burden, such CNAs may serve a more prominent role in shaping tumor biology. This reliance on CNAs, rather than mutations, highlights a potential therapeutic vulnerability unique to this subtype (34,37), and underscores the need for further investigation into the functional significance and targetability of these genes.

Prognostic role of CD44 expression in the claudin-low breast cancer subtype. Kaplan-Meier survival curves based on the METABRIC dataset showed the subtype-specific associations of CD44 expression with overall survival. In the claudin-low subtype, low CD44 expression was associated with improved survival ($P=0.0419$), whereas in the luminal B subtype, low CD44 expression was associated with poor outcomes ($P=0.0053$). By contrast, no significant survival differences were observed between the high and low CD44 expression groups in patients with the basal, luminal A and HER2 subtypes (Fig. 2). These findings suggested that the prognostic value of CD44 was subtype-specific, highlighting

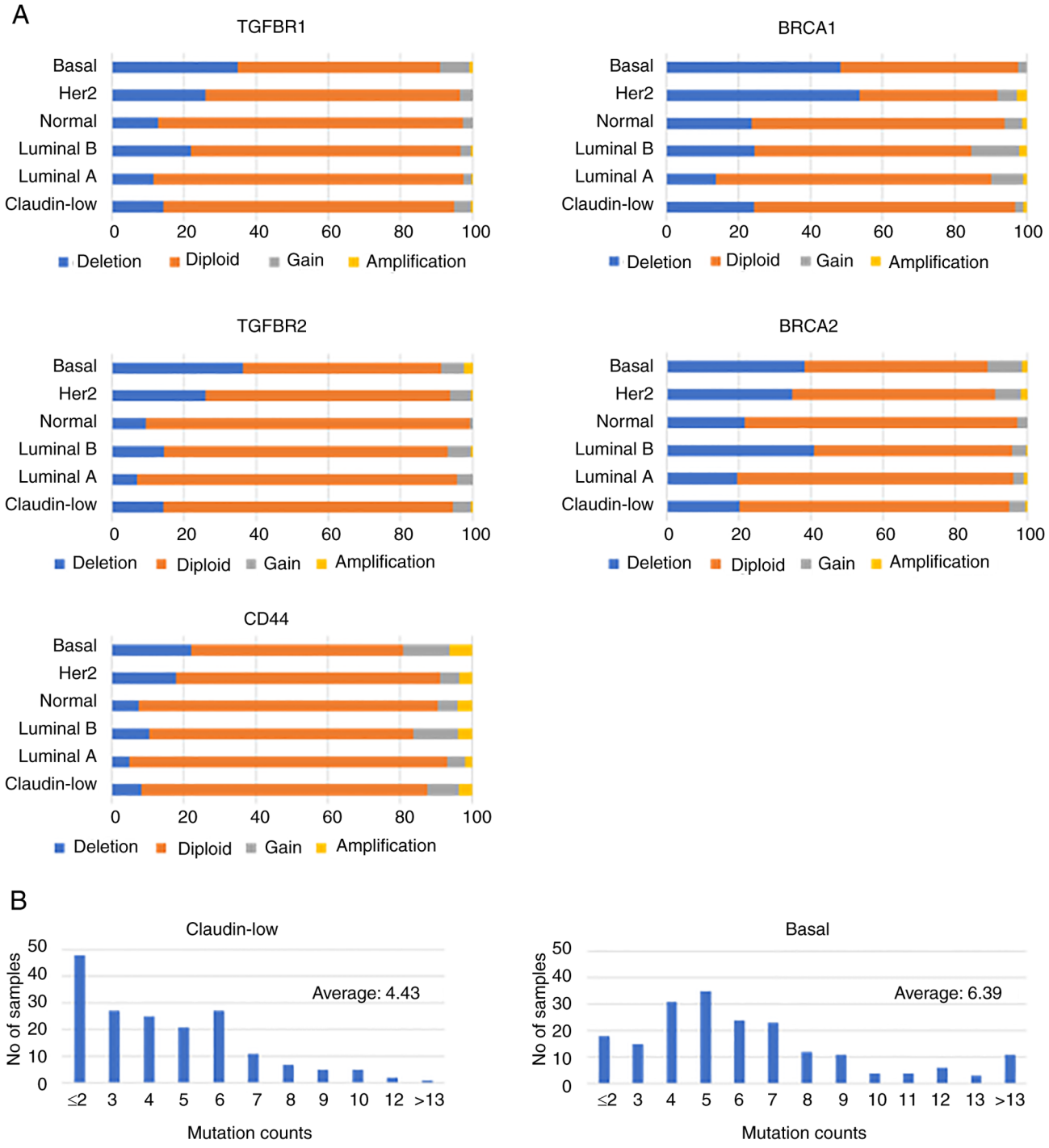

Figure 1. CNAs and mutation burden across breast cancer subtypes (METABRIC dataset). (A) Bar plots showing the distribution of CNAs for TGFBR1, TGFBR2, CD44, BRCA1 and BRCA2 across breast cancer subtypes (claudin-low, luminal A, luminal B, Her2-enriched, basal and normal-like) based on the METABRIC dataset. CNAs were categorized as deletions (blue), diploid (orange), gains (gray) and amplifications (yellow). (B) Histogram representing the distribution of mutation counts in claudin-low (n=179) and basal (n=197) breast cancer samples based on the METABRIC dataset. Claudin-low tumors exhibited a significantly lower mutational burden (mean ± SD, 4.43±2.70) compared with basal tumors (mean ± SD, 6.39±3.84) (Mann-Whitney U test; P<0.0001). CNA, copy number alteration; TGFBR, TGF-β receptor.

the importance of considering the breast cancer subtype when evaluating CD44 as a prognostic biomarker or therapeutic target. This indicated that CD44-targeted strategies should be tailored to the molecular subtype of the tumor.

Dual targeting of CD44 and TGF-β signaling suppresses viability and invasion in claudin-low breast cancer cells. The effects of multiple TGFBR inhibitors, including LY-61, SB431542 and Galunisertib, on the viability of various breast cancer cell lines (SUM159, MDA-MB-231 and MDA-MB-468) were evaluated. Among these, LY-61 showed the most pronounced inhibitory effect on viability, particularly in claudin-low subtype cell lines such as SUM159 and MDA-MB-231 cells, in which its effects were statistically significant compared with the control. By contrast, the basal-like cell line MDA-MB-468 exhibited minimal sensitivity to these

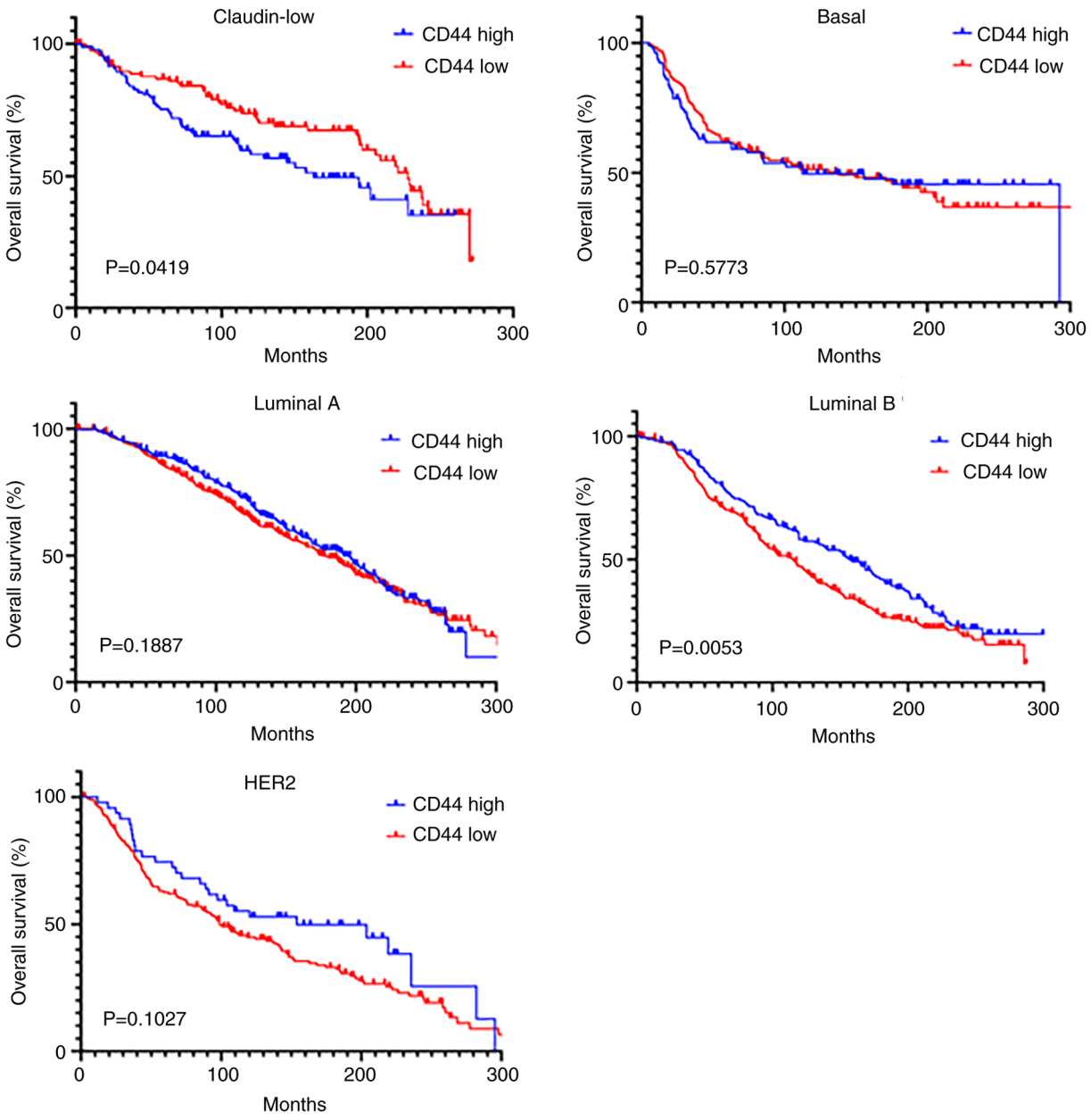

Figure 2. Kaplan-Meier survival curves for overall survival based on CD44 expression across breast cancer subtypes (METABRIC dataset). Kaplan-Meier curves showing overall survival based on CD44 expression levels (high, blue; low, red) across breast cancer subtypes. Statistical comparisons were performed using the log-rank test. Significant differences in survival were observed in the claudin-low (P=0.0419) and luminal B (P=0.0053) subtypes. No statistically significant differences were noted in the basal, luminal A and HER2-enriched subtypes.

inhibitors (Fig. 3A). These findings demonstrated that LY-61 potently inhibited cell viability in claudin-low breast cancer cell lines.

To validate CD44 knockdown, reduced CD44 expression was confirmed using western blot analysis in SUM159 and MDA-MB-231 cells (Fig. 3B). Further experiments combining LY-61 treatment with CD44 knockdown demonstrated an enhanced inhibitory effect on both cell viability (Fig. 3C) and colony formation (Fig. 3D) compared with either treatment alone. Representative images of colony formation in SUM159 and MDA-MB-231 cells are shown in Fig. S1A. CD44 knockdown and LY-61 treatment individually suppressed viability and colony formation to a similar extent; however, their combination resulted in a more pronounced reduction in both parameters. Although individual comparisons showed significant differences between treatment groups, no statistically significant interaction was detected in the two-way ANOVA, suggesting an additive rather than synergistic effect.

In the invasion assays (Fig. 3E), both SUM159 and MDA-MB-231 cells were examined. LY-61 treatment markedly reduced invasion in both cell lines, whereas CD44 knockdown alone had a minimal impact. This suggested that LY-61 was particularly effective in impairing the invasive behavior of cancer cells, likely through mechanisms independent of CD44.

Collectively, these findings indicated that although CD44 knockdown effectively suppressed cell viability and colony formation in SUM159 and MDA-MB-231 cells, it had a limited effect on cell invasion. By contrast, LY-61 treatment consistently inhibited proliferative and invasive behaviors in

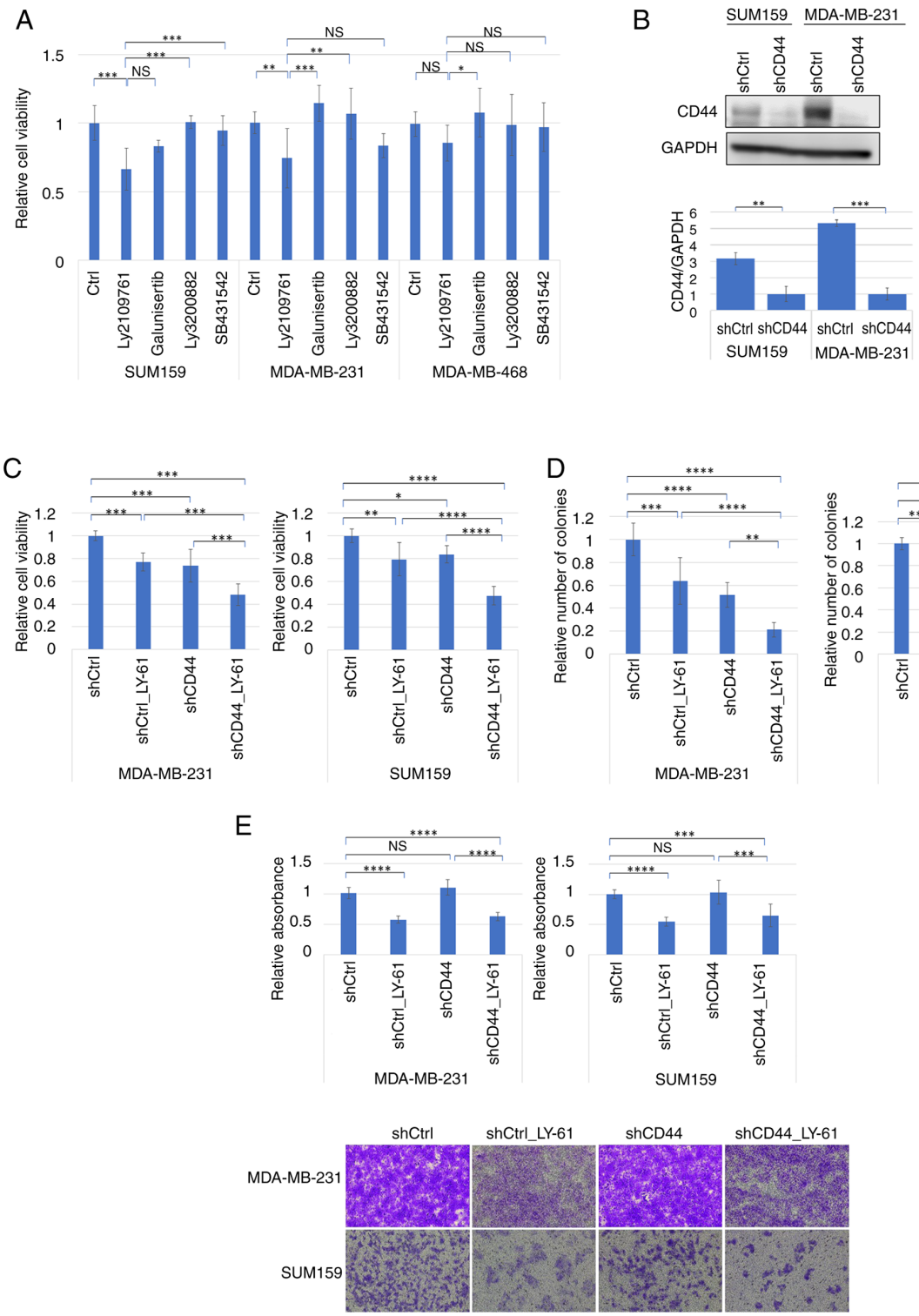

Figure 3. Additive antitumor effects of LY-61 and CD44 knockdown in claudin-low breast cancer cell lines. (A) Relative viability of breast cancer cell lines (SUM159, MDA-MB-231 and MDA-MB-468) following treatment with TGF-β receptor inhibitors (LY-61, Ly3200882, SB431542 and Galunisertib; all at 10 μM). Cells (1,000 per well) were plated in 96-well plates, and drugs were added 24 h after plating. Cell viability was measured using the MTT assay on day 5 after plating. Statistical comparisons were made using one-way ANOVA followed by Tukey's multiple comparisons test for each cell line. (B) Western blot analysis of CD44 expression in SUM159 and MDA-MB-231 cells following shRNA transduction. Densitometric semi-quantification of CD44 protein levels relative to GAPDH is shown below the blots (n=3). Data are presented as the mean ± SD. Statistical comparisons were performed using unpaired two-tailed t-tests. (C) Relative viability of MDA-MB-231 and SUM159 cells following CD44 knockdown (shCD44) and/or treatment with LY-61 (10 μM). Cells (1,000 per well) were plated in 96-well plates, and LY-61 was added 24 h after plating. Cell viability was determined using an MTT assay on day 5 after plating. Statistical significance was assessed using two-way ANOVA followed by Tukey's multiple comparisons test. (D) Colony formation assays showing relative colony numbers in MDA-MB-231 and SUM159 cells following CD44 knockdown and/or LY-61 treatment. Statistical comparisons were performed using two-way ANOVA followed by Tukey's multiple comparisons test. (E) Invasion assays in SUM159 and MDA-MB-231 cells showing the relative absorbance and representative microscopy images of invaded cells stained on the underside of basement membrane matrix-coated inserts. Cells were treated with LY-61 and/or subjected to CD44 knockdown. Statistical analysis was performed using two-way ANOVA followed by Tukey's multiple comparisons test. Representative images are shown at a magnification of x100. (A and C-E) Data are presented as the mean ± SD of three independent experiments (n=3). *P<0.05; **P<0.01; ***P<0.001; ****P<0.0001. Ctrl, control; LY-61, LY2109761; NS, not significant; sh/shRNA, short hairpin RNA.

both cell lines. Notably, the combination of CD44 knockdown and LY-61 treatment led to greater suppression of cell viability and colony formation, and also reduced the invasive capacity compared with that in the shCtrl group without LY-61 treatment, the latter effect being primarily attributable to LY-61. These results highlight the complementary effects of targeting CD44 and TGF-β signaling in claudin-low breast cancer cells.

LY-61 attenuates CD44 knockdown-mediated activation of the TGF-β/Smad2 pathway. The STRING network analysis (Fig. S1B) revealed a strong interaction between CD44 and TGFBR1, suggesting that CD44 serves a potential regulatory role in TGF-β signaling. This association was confirmed by co-immunoprecipitation assays (Fig. 4A), as CD44 and TGFBR1 co-precipitated in control cells transduced with non-targeting shRNA (shCtrl); however, this interaction was lost following CD44 knockdown. These findings indicated that CD44 may modulate TGF-β signaling through TGFBR1 by influencing receptor stability or complex formation.

Western blot analysis (Fig. 4B) showed that Smad2 protein levels were not notably altered by LY-61 treatment or CD44 knockdown alone in both MDA-MB-231 and SUM159 cells. However, a modest decrease in Smad2 protein levels was observed following combined treatment. Consistently, the results shown in Fig. S1C confirmed efficient CD44 knockdown and showed no marked changes in TGFBR1 or TGFBR2 expression. This pattern was also reflected in the RT-qPCR results, where Smad2 mRNA levels showed a similar downward trend following combined treatment. These findings suggested that dual inhibition exerted a cumulative suppressive effect on Smad2 expression, although the magnitude of the change remained limited.

A crucial observation was the impact of CD44 knockdown on Smad2 phosphorylation (p-Smad2) in response to TGF-β stimulation (Fig. 4C). In the MDA-MB-231 and SUM159 cells, TGF-β treatment markedly increased the p-Smad2 levels. CD44 knockdown alone did not induce Smad2 phosphorylation; however, it enhanced TGF-β-induced Smad2 phosphorylation compared with that in shCtrl cells, indicating increased sensitivity to TGF-β signaling. Notably, LY-61 treatment markedly inhibited TGF-β-induced Smad2 phosphorylation (Fig. 4D), demonstrating its potent inhibitory effect on Smad2 activation, regardless of CD44 expression.

To assess whether CD44 knockdown affects TGF-β-induced EMT, the expression levels of the EMT-related transcription factors *Snai1* and *Twist* were subsequently examined. As shown in Fig. 4E, CD44 knockdown significantly increased *Snai1* and *Twist* mRNA expression in SUM159 cells ($P<0.05$), whereas only a non-significant upward trend was observed in MDA-MB-231 cells. In MDA-MB-231 cells, LY-61 monotherapy (shCtrl_LY-61) significantly downregulated *Snai1* expression ($P<0.05$), while *Twist* expression remained unchanged. Notably, treatment with LY-61 significantly reduced *Snai1* expression in CD44-knockdown MDA-MB-231 cells ($P<0.01$), whereas *Twist* showed a non-significant downward trend. In SUM159 cells, LY-61 significantly suppressed both *Snai1* and *Twist* expression in the context of CD44 knockdown ($P<0.05$). These findings suggested that LY-61 counteracted TGF-β/Smad2-mediated EMT transcriptional activity, even under conditions of CD44 knockdown, as shown by its suppression of TGF-β-induced Smad2 phosphorylation (Fig. 4D) and the concomitant reduction of *Snai1* and *Twist* expression in LY-61-treated CD44-knockdown cells compared with untreated CD44-knockdown cells (Fig. 4E). Consistently, LY-61 also reduced Snai1 protein levels in CD44-knockdown SUM159 cells, with the combination group (shCD44_LY-61) showing the lowest Snai1/GAPDH ratio. By contrast, CD44 knockdown alone did not significantly increase Snai1 expression (Fig. S1D).

These findings suggested that CD44 knockdown did not directly enhance Smad2 phosphorylation but increased EMT-related gene expression, indicating that CD44 may influence TGFBR1-mediated signaling rather than Smad2 activation itself. LY-61 effectively inhibited Smad2 phosphorylation and suppressed EMT marker expression, highlighting its potential to counteract TGF-β-driven invasive behavior in claudin-low breast cancer.

Cell line-specific effects of LY-61 and CD44 knockdown on the cell cycle and apoptosis in claudin-low breast cancer cells. In SUM159 cells, LY-61 treatment increased the proportion of cells in the S phase under both control (shCtrl_LY-61) and CD44-knockdown conditions (shCD44_LY-61), suggesting delayed DNA replication and potential checkpoint activation rather than full cell cycle arrest (38). Furthermore, G_2 phase accumulation was observed following CD44 knockdown in SUM159 cells, suggesting that CD44 loss may contribute to delayed cell cycle progression at G_2. By contrast, MDA-MB-231 cells showed only a slight increase in the S phase fraction after LY-61 treatment, and CD44 knockdown exerted a negligible effect on G_2 phase distribution, indicating that the influence of CD44 on cell cycle regulation differed between these two cell lines (Fig. 5A and B).

Apoptosis assays (Fig. 5C and D) revealed that CD44 knockdown increased apoptosis, as indicated by a higher percentage of annexin V-positive cells compared with the shCtrl group. This suggested that CD44 knockdown compromised tumor cell survival by enhancing apoptotic signaling. Western blotting further showed that CD44 knockdown decreased Bcl-2 protein levels in MDA-MB-231 cells, although the reduction was not statistically significant (Fig. S1E), suggesting a role of CD44 in pro-survival signaling via Bcl-2 regulation.

When LY-61 treatment was combined with CD44 knockdown (shCD44_LY-61), the percentage of apoptotic cells remained increased compared with that in the shCtrl group but was slightly reduced compared with that following CD44 knockdown alone in SUM159 cells, while in MDA-MB-231 cells it was higher than that in the shCtrl group and similar to that in the CD44 knockdown group. These findings suggest that LY-61 treatment and CD44 inhibition acted through distinct but complementary mechanisms to suppress tumor cell survival. LY-61 mainly affected cell cycle progression by inducing S phase accumulation, particularly in SUM159 cells, whereas CD44 knockdown increased apoptosis, thereby reducing the overall proliferative capacity.

These findings highlighted the cell line-specific effects of LY-61 and CD44 knockdown on cell cycle progression and apoptosis. LY-61-mediated S phase accumulation was pronounced in SUM159 cells but only slight in MDA-MB-231 cells, underscoring the context-dependent nature of cell cycle

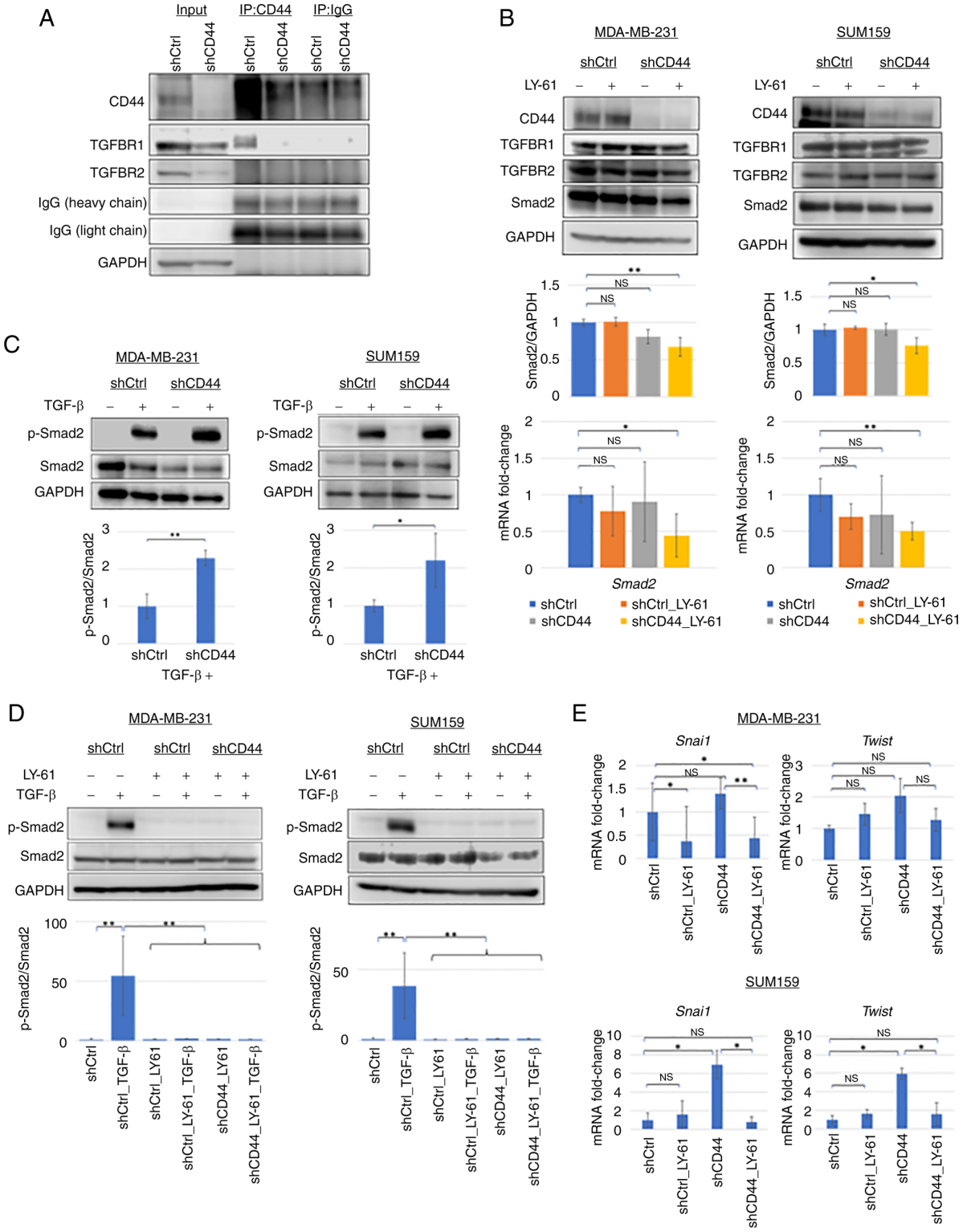

Figure 4. Effects of LY-61 and CD44 knockdown on the TGF-β/Smad2 pathway in claudin-low breast cancer cell lines. (A) Co-immunoprecipitation assays showing that CD44 co-precipitated with TGFBR1 in MDA-MB-231 cells. The CD44-TGFBR1 interaction signal was reduced in shCD44 cells. No detectable co-precipitation was observed between CD44 and TGFBR2. (B) Western blotting and RT-qPCR showing Smad2 protein and mRNA levels in MDA-MB-231 and SUM159 cells following CD44 knockdown and/or LY-61 treatment. Representative western blots (top), densitometric semi-quantification of Smad2 protein levels (middle) and mRNA expression levels determined by RT-qPCR (bottom) are shown. Data are presented as the mean ± SD from three independent experiments (n=3). (C) Western blot analysis of p-Smad2 and total Smad2 protein levels after TGF-β stimulation in MDA-MB-231 and SUM159 cells with or without CD44 knockdown. The semi-quantification of Smad2 phosphorylation was performed by calculating the p-Smad2/Smad2 ratio. CD44 knockdown increased TGF-β-induced p-Smad2 levels in both cell lines. (D) Western blotting showing the effect of LY-61 treatment on p-Smad2 levels in MDA-MB-231 and SUM159 cells. Densitometric semi-quantification of the p-Smad2/Smad2 ratio from three independent experiments (n=3) is shown below the blots. (E) Relative mRNA expression levels of *Snai1* and *Twist* in SUM159 and MDA-MB-231 cells following CD44 knockdown and/or LY-61 treatment, as determined using RT-qPCR. Data are presented as the mean ± SD from three independent experiments (n=3). Statistical significance was assessed using one-way ANOVA followed by (B) Dunnett's or (D and E) Tukey's multiple comparisons test, or (C) unpaired two-tailed Student's t-test. *P<0.05; **P<0.01. Ctrl, control; LY-61, LY2109761; NS, not significant; p-, phosphorylated; RT-qPCR, reverse transcription-quantitative PCR; sh, short hairpin RNA; *Snai1*, snail family transcriptional repressor 1; TGFBR, TGF-β receptor; IP, immunoprecipitation.

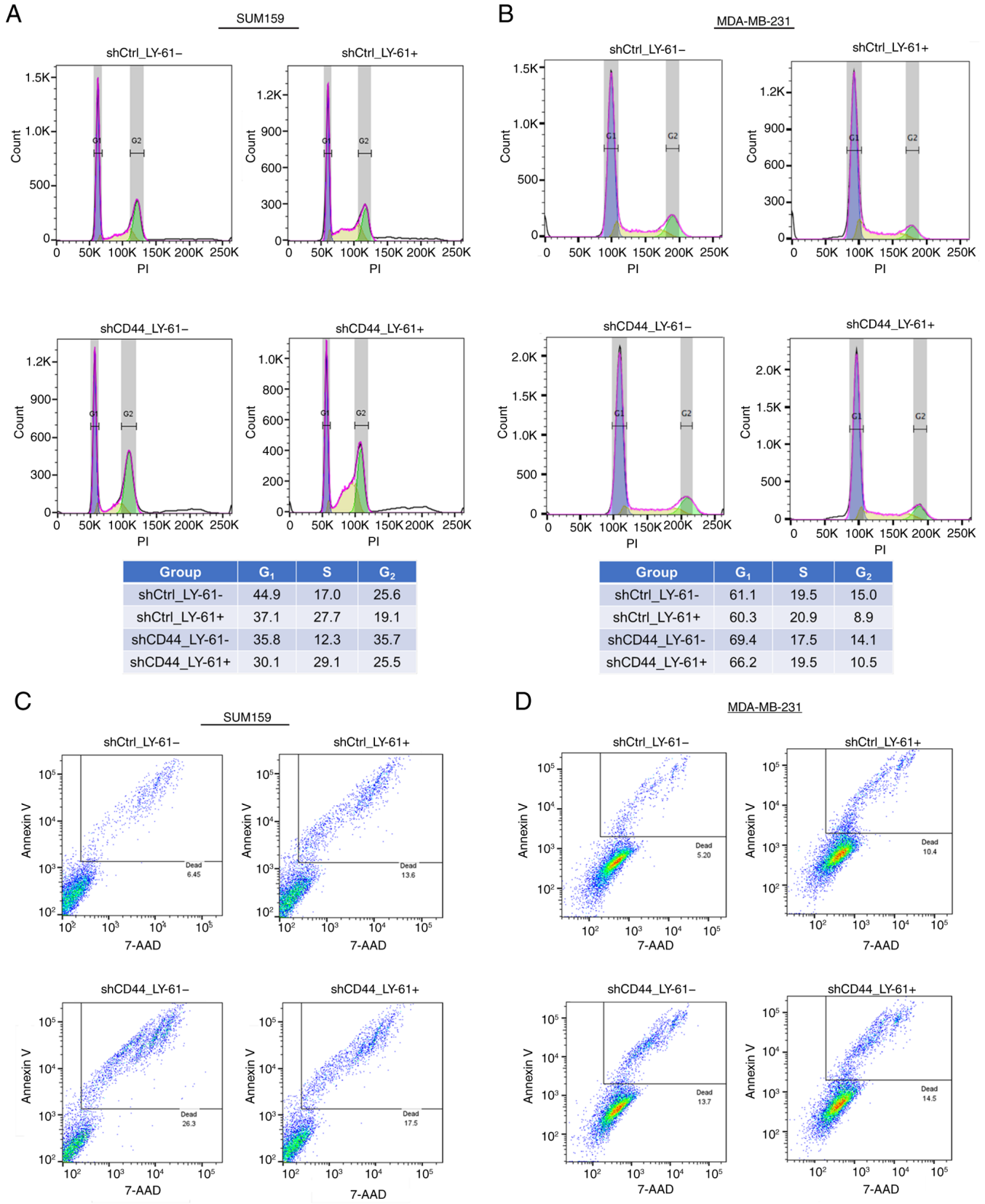

Group	G_1	S	G_2
shCtrl_LY-61-	44.9	17.0	25.6
shCtrl_LY-61+	37.1	27.7	19.1
shCD44_LY-61-	35.8	12.3	35.7
shCD44_LY-61+	30.1	29.1	25.5

Group	G_1	S	G_2
shCtrl_LY-61-	61.1	19.5	15.0
shCtrl_LY-61+	60.3	20.9	8.9
shCD44_LY-61-	69.4	17.5	14.1
shCD44_LY-61+	66.2	19.5	10.5

Figure 5. Effects of LY-61 and CD44 knockdown on cell cycle progression and apoptosis in claudin-low breast cancer cells. (A and B) Flow cytometry analysis of cell cycle distribution in (A) SUM159 and (B) MDA-MB-231 cells treated with LY-61 and/or CD44 knockdown. LY-61 treatment induced S phase accumulation, most prominently in SUM159 cells. In SUM159 cells, CD44 knockdown increased G_2 phase accumulation, suggesting delayed progression through the cell cycle. By contrast, in MDA-MB-231 cells, the proportion of cells in the G_2 phase remained relatively unchanged. The tables summarize the percentages of cells in each phase. Percentages may not total exactly 100% due to the exclusion of sub-G_1 and debris populations and rounding errors (values were rounded to one decimal place after calculation from two decimal places, which may cause minor deviations such as totals slightly >100%). (C and D) Apoptosis analysis using annexin V/7-AAD staining in (C) SUM159 and (D) MDA-MB-231 cells following CD44 knockdown and/or LY-61 treatment. CD44 knockdown increased apoptosis, whereas LY-61 treatment alone had a minimal effect. 7-AAD, 7-aminoactinomycin D; Ctrl, control; LY-61, LY2109761; sh, short hairpin RNA.

regulation in claudin-low breast cancer. Meanwhile, CD44 knockdown consistently increased apoptosis across both cell lines, demonstrating the role of CD44 in supporting tumor cell survival. The combined inhibition of CD44 and TGF-β signaling (via LY-61) is a promising strategy for the simultaneous disruption of proliferation and survival mechanisms in claudin-low breast cancer subtypes.

Discussion

The present study provided novel insights into genomic alterations and potential therapeutic vulnerabilities in the claudin-low breast cancer subtype, with a particular focus on CD44, TGFBR1 and TGFBR2. The present results suggested that claudin-low tumors relied more on CNAs and epigenetic changes than mutations. This pattern was consistent with the lower overall mutational burden observed in claudin-low tumors compared with basal-like tumors, indicating that while mutations are involved, alternative mechanisms, such as CNAs and epigenetic changes, may serve a more prominent role in promoting tumor progression in this subtype (9,34,37). These findings highlight the unique genomic landscape of claudin-low breast cancer, distinct from basal-like tumors, which are characterized by high genomic instability and frequent BRCA1/2 mutations (9,34,37,39). Understanding these subtype-specific differences is crucial for the identification of effective therapeutic targets.

One of the key findings of the present study was the complex role of CD44 in claudin-low breast cancer. While low CD44 expression was associated with improved survival in claudin-low tumors, CD44 knockdown led to significant upregulation of *Snai1* and *Twist* expression in SUM159 cells, whereas only a modest, non-significant increase was observed in MDA-MB-231 cells. This suggests a potential enhancement of EMT-related transcriptional responsiveness. Although previous studies have predominantly reported that CD44 promotes EMT and stemness in various cancer types, including breast cancer (10,28,40-42), some reports suggest that CD44 may also restrain EMT under specific conditions (for example, when differences in the cellular context, microenvironment or signaling network alter its downstream interactions) (10,12-14). The present findings differ from numerous previous reports describing CD44 knockdown as suppressing EMT markers and invasive potential (10,42,28), but may reflect a context-specific response in claudin-low cells. This contradiction indicates that CD44 serves dual roles: Supporting tumor cell survival while modulating TGF-β signaling in a way that restrains EMT. The present results demonstrated that CD44 knockdown increased apoptosis, which may explain the improved prognosis associated with low CD44 expression regardless of its pro-EMT effects. These findings underscore the context-dependent functions of CD44 in claudin-low breast cancer and the importance of considering subtype-specific differences when evaluating CD44 as a biomarker or therapeutic target.

From a therapeutic perspective, the present study demonstrated that LY-61, a TGFBR inhibitor, exerted potent antitumor effects on claudin-low breast cancer cell lines. However, its effects on cell cycle regulation differed between SUM159 and MDA-MB-231 cells. In SUM159 cells, LY-61 induced S phase accumulation and G_2 phase delay, indicating impaired cell cycle progression. By contrast, MDA-MB-231 cells exhibited a slight increase in the S-phase fraction accompanied by a modest reduction in the G_2-phase fraction compared with the control, suggesting that LY-61 did not induce full cell cycle arrest but rather delayed S phase progression in a cell line-dependent manner. These differences may reflect variations in DNA damage response or checkpoint activation (38).

These findings align with the known complexity of TGF-β signaling in breast cancer. Although TGF-β typically induces G_1 arrest via CDK inhibitors, this mechanism is often dysregulated in cancer (35,43). Inhibition of TGF-β signaling may promote S phase entry by bypassing residual G_1 control (24). In the present study, S phase accumulation was observed in both cell lines following LY-61 treatment, but the effect was more pronounced in SUM159 cells, whereas only a slight increase was detected in MDA-MB-231 cells. In both cell lines, LY-61 treatment was accompanied by a comparable reduction in the G_2-phase fraction (from 25.6 to 19.1% in SUM159 cells and from 15.0 to 8.9% in MDA-MB-231 cells), consistent with delayed progression from S to G_2. These results underscore the cell line-specific nature of TGF-β pathway responses and suggest that therapeutic strategies targeting this pathway may need to account for differences in cell cycle regulation.

Aside from affecting cell cycle progression, LY-61 also effectively counteracted the modest EMT-related gene expression changes observed following CD44 knockdown. CD44 knockdown increased *Snai1* and *Twist* expression in SUM159 cells, while the changes were modest in MDA-MB-231 cells. However, LY-61 treatment markedly inhibited TGF-β-induced Smad2 phosphorylation, and also suppressed the expression of *Snai1* and *Twist* compared with that in CD44-knockdown cells without LY-61 treatment, effectively counteracting the pro-invasive signals induced by TGF-β. These findings suggested that while CD44 knockdown may enhance tumor cell plasticity, LY-61 mitigated this effect by inhibiting the key drivers of EMT.

These findings are consistent with previous studies showing that pharmacological inhibition of TGF-β signaling (for example, using SB431542) suppressed Smad2 phosphorylation and downregulated EMT-related transcription factors such as *Snai1* and *Twist*, thereby inhibiting TGF-β-induced invasion in breast cancer cells (36,44,45). Although CD44 has been reported to promote EMT and its knockdown has been reported to suppress EMT markers (28,41,42), the present data revealed a modest increase in *Snai1* and *Twist* expression following CD44 knockdown. This discrepancy may reflect differences in cellular context, such as variations in TGF-β signaling activity or other regulatory pathways. It is possible that, under certain conditions, CD44 knockdown sensitizes cells to TGF-β-induced EMT. This complexity may also help explain why low CD44 expression was not consistently associated with improved prognosis across subtypes, showing a favorable association in claudin-low tumors, but not in basal, luminal A, luminal B or HER2-enriched subtypes. Even in tumors with low CD44 expression, EMT-inducing pathways such as TGF-β signaling may remain active, thereby limiting the survival benefit associated with low CD44 expression (40,46-48).

The present data revealed a functional interplay between CD44 and TGF-β signaling in claudin-low breast cancer.

Co-immunoprecipitation assays in MDA-MB-231 cells demonstrated a physical interaction between CD44 and TGFBR1, and this interaction was lost following CD44 knockdown. These findings suggest that CD44 may exert its role in TGF-β signaling not through the direct modulation of Smad2 phosphorylation, but rather through its interaction with TGFBR1, possibly affecting receptor stability or accessibility to downstream effectors, consistent with a previous study describing the functional relevance of CD44 in TGF-β receptor regulation (26). Although SUM159 cells also exhibit claudin-low characteristics, CD44 knockdown and LY-61 treatment did not induce an apparent reduction in TGFBR1 and TGFBR2 protein levels, whereas MDA-MB-231 cells showed a tendency toward decreased TGFBR2 expression, while TGFBR1 levels remained largely unchanged. This difference may reflect subtle, cell line-specific variations in the regulation of TGFBR stability or turnover. It should be noted that the CD44-TGFBR1 interaction was assessed only in MDA-MB-231 cells; thus, further studies are required to determine whether similar mechanisms operate in SUM159 cells.

While CD44 knockdown alone markedly increased apoptosis, the combination of LY-61 and CD44 knockdown resulted in comparable or slightly lower apoptosis levels than CD44 knockdown alone; however, apoptosis remained elevated compared with shCtrl cells. This suggested that LY-61 and CD44 inhibition acted through distinct but complementary mechanisms. CD44 depletion increased apoptosis by disrupting survival signaling, whereas LY-61 delayed cell cycle progression, which may reduce apoptotic stress in a compensatory manner. Although LY-61 reduced the level of apoptosis observed compared with CD44 knockdown alone in SUM159 cells, no such decrease was observed in MDA-MB-231 cells. Nevertheless, combined treatment with LY-61 and CD44 knockdown effectively suppressed both proliferation and invasion compared with those in the shCtrl group without LY-61 treatment, suggesting a complementary therapeutic mechanism.

These results highlighted the complex and potentially dual role of CD44 in claudin-low breast cancer. While CD44 supports tumor survival, it may also restrain EMT by modulating TGF-β signaling, as suggested by the present findings and supported by a previous report demonstrating the regulatory interaction between CD44 and TGFBR1 (26). In the present study, CD44 knockdown increased apoptosis and was associated with a modest upregulation of EMT-related transcription factors such as *Snai1* and *Twist*, possibly reflecting a compensatory response to the loss of survival signaling. These findings are consistent with previous reports showing that CD44 promoted cancer stemness and may suppress EMT under certain conditions (10,11), whereas other studies have linked CD44 upregulation to enhanced EMT and metastasis (10,40). It remains to be clarified whether this EMT-related gene expression change is a direct effect of CD44 loss or a secondary adaptation due to disrupted cell survival mechanisms.

The effects of TGFBR inhibition observed in the present study underscore the therapeutic significance of this pathway in claudin-low breast cancer. Prior studies have demonstrated that TGF-β serves a role in mediating EMT, immune evasion and resistance to therapy (36,49). The present results reinforced the notion that selective inhibition of TGF-β signaling, particularly when combined with disruption of CD44-mediated pathways, may represent a promising strategy for managing claudin-low tumors, which currently lack effective treatment options.

The findings of the present study suggest a potential therapeutic strategy for claudin-low breast cancer by targeting the TGF-β/Smad2 pathway (via LY-61) and CD44-mediated survival mechanisms. However, the differential effects of LY-61 on cell cycle progression across claudin-low cell lines underscore the need for further investigation into the molecular determinants of its efficacy.

A key limitation of the present study was the lack of *in vivo* validation. Although the present *in vitro* findings provided strong mechanistic insights into the cooperative effects of CD44 knockdown and TGFBR inhibition, the therapeutic implications of this dual-targeting strategy remain hypothetical. Future studies using xenograft models or patient-derived organoids will be essential to validate these *in vitro* observations in physiologically relevant systems, and to evaluate treatment efficacy, systemic toxicity and interactions within the tumor microenvironment.

Although *in vivo* analyses were beyond the scope of the present study, the present findings offer a valuable preclinical framework. The present study demonstrated how CD44 and TGF-β signaling interacted to regulate proliferation, invasion, EMT and cell survival in claudin-low breast cancer. These insights establish a basis for future translational research aimed at developing combinatorial therapeutic strategies for this aggressive and poorly understood subtype. Additional investigations should also explore potential compensatory signaling pathways that might limit the effectiveness of TGF-β blockade and evaluate the long-term outcomes of Smad2 inhibition *in vivo*.

Aside from the CD44-TGF-β axis investigated in the present study, other EMT-related transcription factors (such as zinc finger E-box binding homeobox 1, forkhead box C2 and Slug) and cancer stemness-associated pathways (such as the Wnt/β-catenin and aldehyde dehydrogenase 1 pathways) may also trigger the malignant phenotype of claudin-low breast cancer (50-53). The present findings demonstrated that dual targeting of CD44 and TGF-β signaling suppressed cell proliferation and invasion, CD44 knockdown increased apoptosis, and LY-61 counteracted EMT-related transcriptional activation. These results support the therapeutic potential of this combinatorial approach and provide a mechanistic basis for further development of more comprehensive treatment approaches.

Although most comparisons using standard statistical methods (such as t-tests and ANOVA) yielded significant results, more advanced multivariate approaches, such as interaction models or multiple regression, could have yielded deeper insights into the interplay among CD44 knockdown, TGF-β inhibition and downstream signaling networks. As such, future studies should incorporate such analyses to better capture the complex relationships among these pathways under varying experimental conditions.

The differential responses observed in SUM159 and MDA-MB-231 cells highlight the need for further mechanistic studies to understand the cell line-specific effects. These differences likely reflect underlying biological heterogeneity within claudin-low breast cancer, including variations in TGFBR expression, downstream signaling responsiveness or EMT status. Additional preclinical studies using a broader

panel of claudin-low cell lines and patient-derived xenografts will be required to validate the generalizability of the present findings and assess their translational relevance.

Acknowledgements

The authors would like to thank Dr Yoshihiro Sowa (Department of Molecular-Targeting Cancer Prevention, Kyoto Prefectural University of Medicine, Kyoto, Japan) and Dr Masahiro Shibata (Department of Breast Surgery, Nagoya Eiseikai Hospital, Nagoya, Japan) for their valuable advice. This abstract was presented at the 2024 San Antonio Breast Cancer Symposium, held on December 10-14, 2024, in San Antonio, TX, USA, and was published as Abstract no. P2-04-06.

Funding

The present study was supported by JSPS KAKENHI (grant no. 21K08612) and the Medical Research Support Project of Shizuoka Prefectural Hospital Organization.

Availability of data and materials

The data generated in the present study may be requested from the corresponding author.

Authors' contributions

RM designed the study. RM and KK performed the experiments and confirmed the authenticity of all the raw data. RM, KK, SI, SS, RH and MT contributed to data analysis and manuscript preparation. All authors have read and approved the final version of the manuscript.

Ethics approval and consent to participate

Not applicable.

Patient consent for publication

Not applicable.

Competing interests

The authors declare that they have no competing interests.

References

1. Dai X, Li T, Bai Z, Yang Y, Liu X, Zhan J and Shi B: Breast cancer intrinsic subtype classification, clinical use and future trends. Am J Cancer Res 5: 2929-2943, 2015.
2. Perou CM, Sørlie T, Eisen MB, van de Rijn M, Jeffrey SS, Rees CA, Pollack JR, Ross DT, Johnsen H, Akslen LA, *et al*: Molecular portraits of human breast tumours. Nature 406: 747-752, 2000.
3. Sørlie T, Perou CM, Tibshirani R, Aas T, Geisler S, Johnsen H, Hastie T, Eisen MB, van de Rijn M, Jeffrey SS, *et al*: Gene expression patterns of breast carcinomas distinguish tumor subclasses with clinical implications. Proc Natl Acad Sci USA 98: 10869-10874, 2001.
4. Xiong X, Zheng LW, Ding Y, Chen YF, Cai YW, Wang LP, Huang L, Liu CC, Shao ZM and Yu KD: Breast cancer: Pathogenesis and treatments. Signal Transduct Target Ther 10: 49, 2025.
5. Herschkowitz JI, Simin K, Weigman VJ, Mikaelian I, Usary J, Hu Z, Rasmussen KE, Jones LP, Assefnia S, Chandrasekharan S, *et al*: Identification of conserved gene expression features between murine mammary carcinoma models and human breast tumors. Genome Biol 8: R76, 2007.
6. Prat A, Parker JS, Karginova O, Fan C, Livasy C, Herschkowitz JI, He X and Perou CM: Phenotypic and molecular characterization of the claudin-low intrinsic subtype of breast cancer. Breast Cancer Res 12: R68, 2010.
7. Sabatier R, Finetti P, Guille A, Adelaide J, Chaffanet M, Viens P, Birnbaum D and Bertucci F: Claudin-low breast cancers: Clinical, pathological, molecular and prognostic characterization. Mol Cancer 13: 228, 2014.
8. Fougner C, Bergholtz H, Norum JH and Sørlie T: Re-definition of claudin-low as a breast cancer phenotype. Nat Commun 11: 1787, 2020.
9. Garrido-Castro AC, Lin NU and Polyak K: Insights into molecular classifications of triple-negative breast cancer: Improving patient selection for treatment. Cancer Discov 9: 176-198, 2019.
10. Hassn Mesrati M, Syafruddin SE, Mohtar MA and Syahir A: CD44: A multifunctional mediator of cancer progression. Biomolecules 11: 1850, 2021.
11. Kim KJ, Godarova A, Seedle K, Kim MH, Ince TA, Wells SI, Driscoll JJ and Godar S: Rb suppresses collective invasion, circulation and metastasis of breast cancer cells in CD44-dependent manner. PLoS One 8: e80590, 2013.
12. Dehbokri SG, Noorolyai S, Baghbani E, Moghaddamneshat N, Javaheri T and Baradaran B: Effects of CD44 siRNA on inhibition, survival, and apoptosis of breast cancer cell lines (MDA-MB-231 and 4T1). Mol Biol Rep 51: 646, 2024.
13. Nam K, Oh S, Lee KM, Yoo SA and Shin I: CD44 regulates cell proliferation, migration, and invasion via modulation of c-Src transcription in human breast cancer cells. Cell Signal 27: 1882-1894, 2015.
14. Yang Z, Chen D, Nie J, Zhou S, Wang J, Tang Q and Yang X: MicroRNA-143 targets CD44 to inhibit breast cancer progression and stem cell-like properties. Mol Med Rep 13: 5193-5199, 2016.
15. Montgomery N, Hill A, McFarlane S, Neisen J, O'Grady A, Conlon S, Jirstrom K, Kay EW and Waugh DJ: CD44 enhances invasion of basal-like breast cancer cells by upregulating serine protease and collagen-degrading enzymatic expression and activity. Breast Cancer Res 14: R84, 2012.
16. Ouhtit A, Madani S, Gupta I, Shanmuganathan S, Abdraboh ME, Al-Riyami H, Al-Farsi YM and Raj MH: TGF-β2: A novel target of CD44-promoted breast cancer invasion. J Cancer 4: 566-572, 2013.
17. Xu H, Niu M, Yuan X, Wu K and Liu A: CD44 as a tumor biomarker and therapeutic target. Exp Hematol Oncol 9: 36, 2020.
18. Zhou L, Sheng D, Deng Q, Wang D and Liu S: Development of a novel method for rapid cloning of shRNA vectors, which successfully knocked down CD44 in mesenchymal triple-negative breast cancer cells. Cancer Commun (Lond) 38: 57, 2018.
19. Huang P, Chen A, He W, Li Z, Zhang G, Liu Z, Liu G, Liu X, He S, Xiao G, *et al*: BMP-2 induces EMT and breast cancer stemness through Rb and CD44. Cell Death Discov 3: 17039, 2017.
20. Gao F, Zhang G, Liu Y, He Y, Sheng Y, Sun X, Du Y and Yang C: Activation of CD44 signaling in leader cells induced by tumor-associated macrophages drives collective detachment in luminal breast carcinomas. Cell Death Dis 13: 540, 2022.
21. Pan C, Xu A, Ma X, Yao Y, Zhao Y, Wang C and Chen C: Research progress of Claudin-low breast cancer. Front Oncol 13: 1226118, 2023.
22. Pommier RM, Sanlaville A, Tonon L, Kielbassa J, Thomas E, Ferrari A, Sertier AS, Hollande F, Martinez P, Tissier A, *et al*: Comprehensive characterization of claudin-low breast tumors reflects the impact of the cell-of-origin on cancer evolution. Nature Commun 11: 3431, 2020.
23. Gooding AJ and Schiemann WP: Epithelial-mesenchymal transition programs and cancer stem cell phenotypes: Mediators of breast cancer therapy resistance. Mol Cancer Res 18: 1257-1270, 2020.
24. Akhurst RJ and Hata A: Targeting the TGFβ signalling pathway in disease. Nat Revi Drug Discov 11: 790-811, 2012.
25. Matsunuma R, Chan DW, Kim BJ, Singh P, Han A, Saltzman AB, Cheng C, Lei JT, Wang J, Roberto da Silva L, *et al*: DPYSL3 modulates mitosis, migration, and epithelial-to-mesenchymal transition in claudin-low breast cancer. Proc Natl Acad Sci USA 115: E11978-E11987, 2018.

26. Porsch H, Mehić M, Olofsson B, Heldin P and Heldin CH: Platelet-derived growth factor β-receptor, transforming growth factor β type I receptor, and CD44 protein modulate each other's signaling and stability. J Biol Chem 289: 19747-19757, 2014.
27. Yang K and Yi T: Tumor cell stemness in gastrointestinal cancer: Regulation and targeted therapy. Front Mol Biosci 10: 1297611, 2023.
28. Chen C, Zhao S, Karnad A and Freeman JW: The biology and role of CD44 in cancer progression: Therapeutic implications. J Hematol Oncol 11: 64, 2018.
29. Flanagan L, Van Weelden K, Ammerman C, Ethier SP and Welsh J: SUM-159PT cells: A novel estrogen independent human breast cancer model system. Breast Cancer Res Treat 58: 193-204, 1999.
30. Livak KJ and Schmittgen TD: Analysis of relative gene expression data using real-time quantitative PCR and the 2(-Delta Delta C(T)) Method. Methods 25: 402-408, 2001.
31. Chan DW, Mody CH, Ting NS and Lees-Miller SP: Purification and characterization of the double-stranded DNA-activated protein kinase, DNA-PK, from human placenta. Biochem Cell Biol 74: 67-73, 1996.
32. Curtis C, Shah SP, Chin SF, Turashvili G, Rueda OM, Dunning MJ, Speed D, Lynch AG, Samarajiwa S, Yuan Y, *et al*: The genomic and transcriptomic architecture of 2,000 breast tumours reveals novel subgroups. Nature 486: 346-352, 2012.
33. Szklarczyk D, Gable AL, Lyon D, Junge A, Wyder S, Huerta-Cepas J, Simonovic M, Doncheva NT, Morris JH, Bork P, *et al*: STRING v11: Protein-protein association networks with increased coverage, supporting functional discovery in genome-wide experimental datasets. Nucleic Acids Res 47: D607-D613, 2019.
34. Voutsadakis IA: Molecular characteristics and therapeutic vulnerabilities of claudin-low breast cancers derived from cell line models. Cancer Genomics Proteomics 20: 539, 2023.
35. Donovan J and Slingerland J: Transforming growth factor-beta and breast cancer: Cell cycle arrest by transforming growth factor-beta and its disruption in cancer. Breast Cancer Res 2: 116-124, 2000.
36. Wang X, Eichhorn PJA and Thiery JP: TGF-β, EMT, and resistance to anti-cancer treatment. Semin Cancer Biol 97: 1-11, 2023.
37. Fougner C, Bergholtz H, Kuiper R, Norum JH and Sørlie T: Claudin-low-like mouse mammary tumors show distinct transcriptomic patterns uncoupled from genomic drivers. Breast Cancer Res 21: 85, 2019.
38. Barcellos-Hoff MH and Gulley JL: Molecular pathways and mechanisms of TGFβ in cancer therapy. Clin Cancer Res 29: 2025-2033, 2023.
39. Kwei KA, Kung Y, Salari K, Holcomb IN and Pollack JR: Genomic instability in breast cancer: Pathogenesis and clinical implications. Mol Oncol 4: 255-266, 2010.
40. Xu H, Tian Y, Yuan X, Wu H, Liu Q, Pestell RG and Wu K: The role of CD44 in epithelial-mesenchymal transition and cancer development. Onco Targets Ther 8: 3783-3792, 2015.
41. Li L, Qi L, Liang Z, Song W, Liu Y, Wang Y, Sun B, Zhang B and Cao W: Transforming growth factor-β1 induces EMT by the transactivation of epidermal growth factor signaling through HA/CD44 in lung and breast cancer cells. Int J Mol Med 36: 113-122, 2015.
42. Gao Y, Ruan B, Liu W, Wang J, Yang X, Zhang Z, Li X, Duan J, Zhang F, Ding R, *et al*: Knockdown of CD44 inhibits the invasion and metastasis of hepatocellular carcinoma both in vitro and in vivo by reversing epithelial-mesenchymal transition. Oncotarget 6: 7828-7837, 2015.
43. Deng Z, Fan T, Xiao C, Tian H, Zheng Y, Li C and He J: TGF-β signaling in health, disease and therapeutics. Signal Transduct Target Ther 9: 61, 2024.
44. Chanmee T, Ontong P, Mochizuki N, Kongtawelert P, Konno K and Itano N: Excessive hyaluronan production promotes acquisition of cancer stem cell signatures through the coordinated regulation of Twist and the transforming growth factor β (TGF-β)-Snail signaling axis. J Biol Chem 289: 26038-26056, 2014.
45. Zhang K, Liu X, Hao F, Dong A and Chen D: Targeting TGF-β1 inhibits invasion of anaplastic thyroid carcinoma cell through SMAD2-dependent S100A4-MMP-2/9 signalling. Am J Transl Res 8: 2196-2209, 2016.
46. Katsuno Y, Meyer DS, Zhang Z, Shokat KM, Akhurst RJ, Miyazono K and Derynck R: Chronic TGF-β exposure drives stabilized EMT, tumor stemness, and cancer drug resistance with vulnerability to bitopic mTOR inhibition. Sci Signal 12: eaau8544, 2019.
47. Ouhtit A, Madani S, Gupta I, Shanmuganathan S, Abdraboh ME, Al-Riyami H, Al-Farsi YM and Raj MH: TGF-β2: A novel target of CD44-promoted breast cancer invasion. J Cancer 4: 566-572, 2013.
48. Park NR, Cha JH, Jang JW, Bae SH, Jang B, Kim JH, Hur W, Choi JY and Yoon SK: Synergistic effects of CD44 and TGF-β1 through AKT/GSK-3β/β-catenin signaling during epithelial-mesenchymal transition in liver cancer cells. Biochem Biophys Res Commun 477: 568-574, 2016.
49. Hao Y, Baker D and Ten Dijke P: TGF-β-mediated epithelial-mesenchymal transition and cancer metastasis. Int J Mol Sci 20: 2767, 2019.
50. Voutsadakis IA: EMT Features in Claudin-Low versus Claudin-Non-Suppressed Breast Cancers and the Role of Epigenetic Modifications. Curr Issues Mol Biol 45: 6040-6054, 2023.
51. Werden SJ, Sphyris N, Sarkar TR, Paranjape AN, LaBaff AM, Taube JH, Hollier BG, Ramirez-Peña EQ, Soundararajan R, den Hollander P, *et al*: Phosphorylation of serine 367 of FOXC2 by p38 regulates ZEB1 and breast cancer metastasis, without impacting primary tumor growth. Oncogene 35: 5977-5988, 2016.
52. Taube JH, Herschkowitz JI, Komurov K, Zhou AY, Gupta S, Yang J, Hartwell K, Onder TT, Gupta PB, Evans KW, *et al*: Core epithelial-to-mesenchymal transition interactome gene-expression signature is associated with claudin-low and metaplastic breast cancer subtypes. Proc Natl Acad Sci USA 107: 15449-15454, 2010.
53. Liang H, Benard O, Kumar V, Griffen A, Ren Z, Sivalingam K, Wang J, de Simone Benito E, Zhang X, Zhang J, *et al*: Wnt/ERK/CDK4/6 activation in the partial EMT state coordinates mammary cancer stemness with self-renewal and inhibition of differentiation. Br J Cancer 133: 986-1002, 2025.